

Optical Engineering

OpticalEngineering.SPIEDigitalLibrary.org

Time–frequency-varying multicarrier generation using dynamic recirculating frequency shifter

Zhipei Li
Bo Liu
Qi Zhang
Xishuo Wang
Yaya Mao
Xiangjun Xin

Time–frequency-varying multicarrier generation using dynamic recirculating frequency shifter

Zhipei Li,^{a,b} Bo Liu,^{c,*} Qi Zhang,^{a,b} Xishuo Wang,^{a,b} Yaya Mao,^c and Xiangjun Xin^{a,b}

^aBeijing University of Posts and Telecommunications, School of Electronic Engineering, Beijing, China

^bBeijing University of Posts and Telecommunications, Beijing Key Laboratory of Space-ground Interconnection and Convergence, Beijing, China

^cNanjing University of Information Science and Technology, Institute of Optoelectronics, Nanjing, China

Abstract. A time–frequency-varying multicarrier generation scheme based on dynamic single-sideband recirculating frequency shifter is proposed and experimentally demonstrated. Through the use of two time-domain sinusoidal signals with stationary phase shift provided by a phase control module, multicarriers with flexible frequency intervals are obtained without carrier-to-noise ratio and flatness loss. We have experimentally attained multicarriers with 10-/12.5-/15-GHz carrier intervals in 3-nm bandwidth, and carriers with arbitrary intervals can be achieved when using the proposed scheme combined with a flexible wavelength selective switch. © The Authors. Published by SPIE under a Creative Commons Attribution 4.0 Unported License. Distribution or reproduction of this work in whole or in part requires full attribution of the original publication, including its DOI. [DOI: 10.1117/1.OE.58.5.056116]

Keywords: multicarrier; single-side-band; recirculating frequency shifter; wavelength selective switch.

Paper 190212 received Feb. 17, 2019; accepted for publication Apr. 30, 2019; published online May 31, 2019.

1 Introduction

Frequency-locking optical multicarrier has unparalleled advantages in fiber communications and optical sensing applications, such as wavelength division multiplexing (WDM) transmission, optical orthogonal frequency division multiplexing signal generation, spectral measurement, and analysis.^{1–3} For example, an optical multicarrier source with high quality and a large number of carriers is a good candidate to serve as a laser array at the transmitter or a local oscillator array at the receiver side for ultra-high speed and high-spectrum efficiency optical transmission systems. For such applications, highly coherent optical multicarrier sources with stable flatness and uniform power distribution are desirable. Many endeavors have been made on the generation of optical multicarriers, conventional multicarrier sources are mainly based on highly nonlinear fibers,⁴ microring resonators,^{5,6} cascaded modulators,⁷ and recirculating frequency shifter (RFS).⁸

RFS has attracted wide attention in recent years because of its simple structure, low driving voltage, and flat subcarrier. IQ modulator with three direct current (DC) bias controls is widely used to realize the continuous and recirculated single-sideband (SSB) modulation with special frequency spacing. At present, 50 or more stable frequency-locked carriers have been successfully generated,⁹ and many improvement techniques have been proposed to achieve better performance,¹⁰ such as using optical-FIR filter for amplified spontaneous emission noise suppression,¹¹ multifrequency and multichannel shifting method for increasing carrier numbers,¹² and modified modulators to enlarge the carrier-to-carrier spacing,^{13–15} while these methods increase the complexity of the RFS scheme, at the same time, the carrier interval of the proposed methods is fixed due to the stationary frequency of the RF source and the phase shifter. The generated multicarrier frequencies are not selective and therefore cannot be flexibly scheduled.

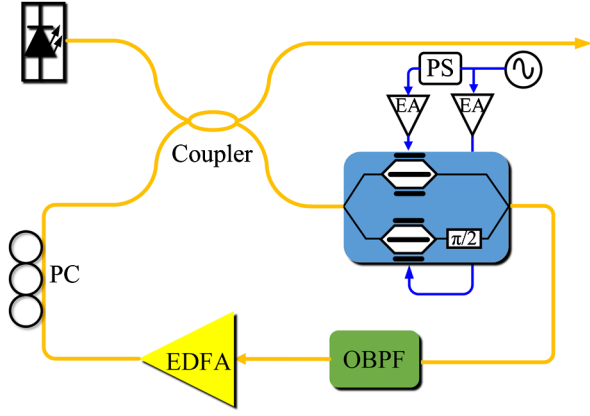
In this paper, we improved the recirculating frequency shifter and proposed a time–frequency-varying multicarrier generation method, by adjusting the delay of two sinusoidal signals in time domain to lock their phase difference, the flexible interval optical multicarriers in frequency domain can be obtained, multicarriers with different carrier spacing have been generated, and two subcarriers can be obtained at any interval. To meet the increasing demand for bandwidth in the future, the scheme is a good candidate for passive-optical-network (PON) integrated with radio-over-fiber (ROF) and photon frequency hopping radar.

2 Principle of Flexible Interval Multicarrier Generation

The structure of the basic RFS is shown in Fig. 1, the RFS consists of a tunable light source that provides the seed carrier of frequency f_0 and a closed fiber loop, which comprises a 50:50 coupler, a radio frequency (RF) signal source, I/Q modulator, an optical bandpass filter (OBPF), which is used to control the number of carriers required, an erbium-doped fiber amplifier (EDFA) to compensate the losses in the loop, and a polarization controller to stabilize the state of polarization.

The I/Q modulator consists of two parallel Mach–Zehnder modulators and a $\pi/2$ phase shifter. In order to make the modulator work in the SSB state and implement carrier frequency shift, two RF signals, which are fed into the I/Q modulator, are supposed to have equal power but $\pi/2$ phase shift. Conventionally, we use an RF signal source to generate a clock signal with the frequency f_s and then split it into two branches, with a phase shifter in one branch to make it $\pi/2$ phase-shifted. Ideally, the input optical field is $E_{in}(t) = A \exp(j2\pi f_0 t)$, the two RF drive signals are $f_I(t) = V_{pp} \sin(2\pi f_s t)$, $f_Q(t) = V_{pp} \sin(2\pi f_s t + \theta)$, where f_s represents the frequency of the RF signal and θ represents the phase difference between two RF signals determined by phase shifter. The electronic field of the I/Q modulator output is represented by Ref. 8:

*Address all correspondence to Bo Liu, E-mail: bo@nuist.edu.cn


Fig. 1 Structure of the RFS.

$$\begin{aligned}
 E_{\text{out}}(t) &= \frac{E_{\text{in}}(t)}{2} \left[j \sin\left(\frac{\pi f_I(t)}{2V_\pi}\right) + \sin\left(\frac{\pi f_Q(t)}{2V_\pi}\right) \right] \\
 &= \frac{E_{\text{in}}(t)}{2} \left\{ j \sin\left[\frac{\pi V_{pp}}{2V_\pi} \sin(2\pi f_s t)\right] \right. \\
 &\quad \left. + \sin\left[\frac{\pi V_{pp}}{2V_\pi} \sin(2\pi f_s t + \theta)\right] \right\}, \quad (1)
 \end{aligned}$$

using the Jacobi–Anger expansion, Eq. (1) can be expressed as follows:

$$\begin{aligned}
 E_{\text{out}}(t) &= \frac{E_{\text{in}}(t)}{2} \{ j \sin[\delta_m \sin(2\pi f_s t)] \\
 &\quad + \sin[\delta_m \sin(2\pi f_s t + \theta)] \} \\
 &= E_{\text{in}}(t) \left\{ j \sum_{k=1}^{\infty} J_{2k-1}(\delta_m) \sin[(2k-1)2\pi f_s t] \right. \\
 &\quad \left. + \sum_{k=1}^{\infty} J_{2k-1}(\delta_m) \sin[(2k-1)(2\pi f_s t + \theta)] \right\} \\
 &= E_{\text{in}}(t) \sum_{k=1}^{\infty} J_{2k-1}(\delta_m) \{ j \sin[(2k-1)2\pi f_s t] \\
 &\quad + \sin[(2k-1)(2\pi f_s t + \theta)] \}, \quad (2)
 \end{aligned}$$

where $\delta_m = \pi V_{pp}/2V_\pi$ denotes the phase modulation depth, and $J_{(2k-1)}(\delta_m)$ is the odd-order Bessel function of the first kind. According to Euler's formula,

$$\begin{aligned}
 E_{\text{out}}(t) &= \frac{E_{\text{in}}(t)}{2} \sum_{k=1}^{\infty} J_{2k-1}(\delta_m) \{ e^{j(2k-1)2\pi f_s t} - e^{-j(2k-1)2\pi f_s t} \\
 &\quad - j[e^{j(2k-1)(2\pi f_s t + \theta)} - e^{-j(2k-1)(2\pi f_s t + \theta)}] \} \\
 &= \frac{E_{\text{in}}(t)}{2} \sum_{k=1}^{\infty} J_{2k-1}(\delta_m) \{ e^{j(2k-1)2\pi f_s t} (1 - j e^{j(2k-1)\theta}) \\
 &\quad + e^{-j(2k-1)2\pi f_s t} (j e^{-j(2k-1)\theta} - 1) \} \\
 &= \frac{E_{\text{in}}(t)}{2} \sum_{k=1}^{\infty} J_{2k-1}(\delta_m) \{ e^{j(2k-1)2\pi f_s t} (-j \cos[(2k-1)\theta] \\
 &\quad + \sin[(2k-1)\theta]) + 1 + e^{-j(2k-1)2\pi f_s t} (j \cos[(2k-1)\theta] \\
 &\quad + \sin[(2k-1)\theta]) - 1 \}, \quad (3)
 \end{aligned}$$

according to the characteristics of Bessel function, the third-order harmonic plays a dominant role among all the harmonics, ignoring all the high-order harmonics beyond the third-order, the output of the RFS after the first round trip (RT) can be expressed as follows:

$$\begin{aligned}
 E_{\text{out}}(t) &\approx \frac{E_{\text{in}}(t)}{2} \{ J_1(\delta_m) [e^{j2\pi f_s t} (-j \cos \theta + \sin \theta + 1) \\
 &\quad + e^{-j2\pi f_s t} (j \cos \theta + \sin \theta - 1)] \\
 &\quad + J_3(\delta_m) [e^{j6\pi f_s t} (-j \cos 3\theta + \sin 3\theta + 1) \\
 &\quad + e^{-j6\pi f_s t} (j \cos 3\theta + \sin 3\theta - 1)] \}. \quad (4)
 \end{aligned}$$

If θ is equal to $\pi/2$, the I/Q modulator works at ideal SSB condition:

$$\begin{aligned}
 E_{\text{out}}(t) &\approx E_{\text{in}}(t) [J_1(\delta_m) e^{j2\pi f_s t} - J_3(\delta_m) e^{-j6\pi f_s t}] \\
 &\approx E_{\text{in}}(t) J_1(\delta_m) [e^{j2\pi f_s t} + c e^{-j6\pi f_s t}], \quad (5)
 \end{aligned}$$

where $c = -J_3(\delta_m)/J_1(\delta_m)$ is the crosstalk coefficient, which depends on drive voltage V_{pp} of the I/Q modulator, we can apply appropriate driving voltage to make $|c| \ll 1$ and the crosstalk of third-order harmonic could be neglected.

When RF is set to 12.5 GHz and I/Q phase difference is $\pi/2$, two RF time-domain signal is shown in Fig. 2(a), where $\theta = 2\pi\Delta T/T$, the I/Q modulator works at perfect SSB condition, optical spectrum after the first RT is shown in Fig. 2(b), λ_0 is seed frequency and λ_1 is the shifted frequency, at this time, we can achieve flat and stable multicarrier when the loop is closed.

In order to achieve flexible interval optical carriers, we need to change the RF frequency f_s while keeping two RF signals $\pi/2$ phase-shifted, but in conventional RFS, the phase shifter is fixed or manual, if we only change the frequency without adjusting the frequency shifter, θ will deviate from $\pi/2$, odd-order negative frequency component will introduce crosstalk and impact the performance of multicarrier. As shown in Fig. 3, when we change RF from 10 to 15 GHz, I/Q phase difference with fixed phase shifter is shown in Fig. 3(a), imperfectly matched RF time-domain signal at 10 and 15 GHz, is shown in Figs. 3(b) and 3(d), optical spectrum after the first RT is shown in Figs. 3(c) and 3(e), at this time, we cannot achieve flat and stable multicarriers when the loop is closed.

To address this problem and achieve multicarriers with high flatness and stability, the RF drive signals are supposed to be perfect balanced. We implement a phase control module, as shown in Fig. 4, which is composed of a digital phase shifter (DPS), an oscilloscope (OSC), a computer, and splitters. The sinusoidal frequency is generated by a RF source and divided into two branches, one branch passes through a DPS while the other is output directly; the OSC collects the time domain signal of the two branches with two power splitters and send it to a computer. We make the computer automatically calculate the phase difference between the two channels and feedback the control message to the DPS. The phase detector keeps working until 90-deg phase difference is detected, in this way, when we change the RF frequency; dynamic adjustments will be made by the phase control module, and two $\pi/2$ phase-shifted RF signals that

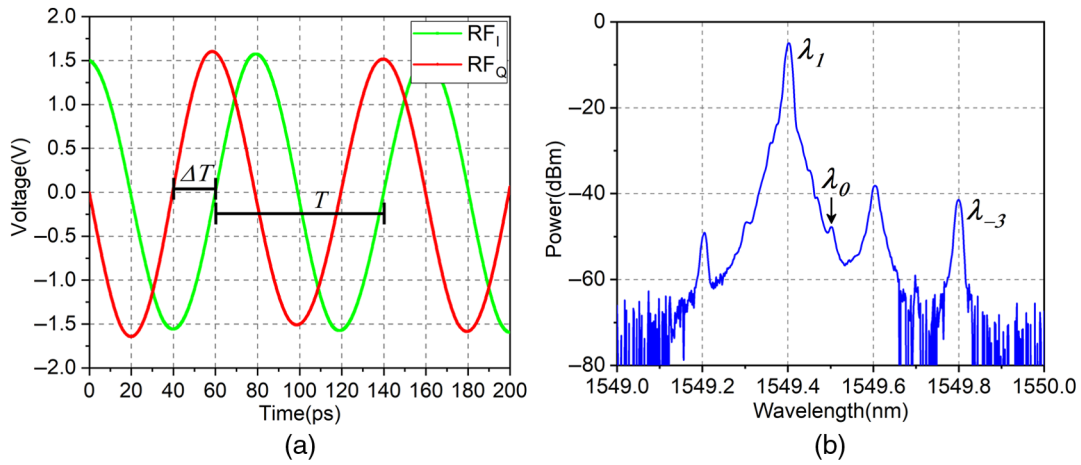


Fig. 2 When θ is equal to $\pi/2$ and RF is 12.5 GHz: (a) RF time-domain signal and (b) optical spectrum after the first RT.

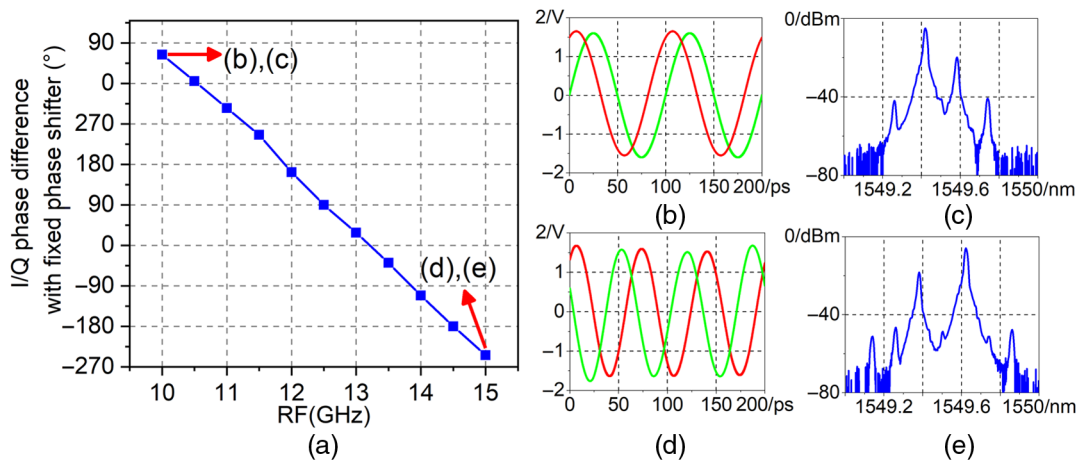


Fig. 3 I/Q phase difference and optical spectrum using fixed phase shifter: (a) I/Q phase difference when RF frequency changes from 10 to 15 GHz, (b) RF time-domain signal at 10 GHz, (c) optical spectrum after first RT at 10 GHz, (d) RF time-domain signal at 15 GHz, and (e) optical spectrum after first RT at 15 GHz.

are obtained in time domain are produced, which leads to the generation of multicarriers with variable interval in frequency domain.

We employ the phase control module in the open loop, as shown in Fig. 5, when RF changes from 10 to 15 GHz, I/Q phase difference is locked at $\pi/2$ by phase control module,

$\pi/2$ phase-shifted time-domain signal at 10, and 15 GHz is shown in Figs. 5(b) and 5(d), and optical spectrum after first RT is shown in Figs. 5(c) and 5(e); the I/Q modulator works at ideal SSB condition and when the loop is closed, multicarriers with flexible interval can be achieved by the dynamic RFS.

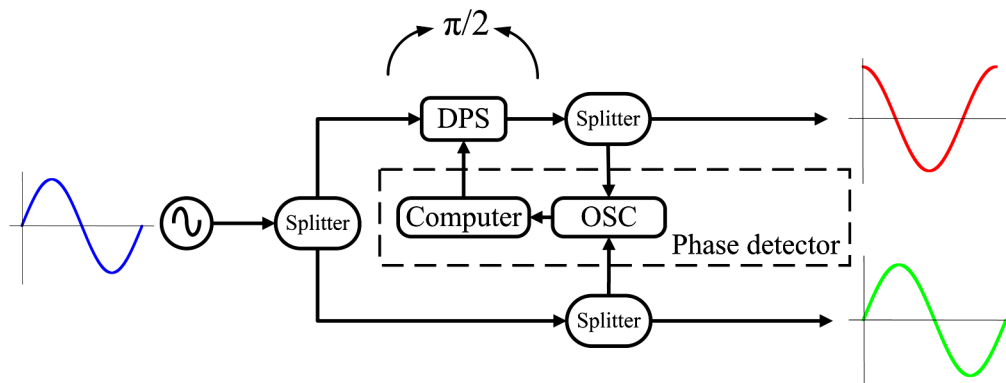


Fig. 4 Structure of the phase control module.

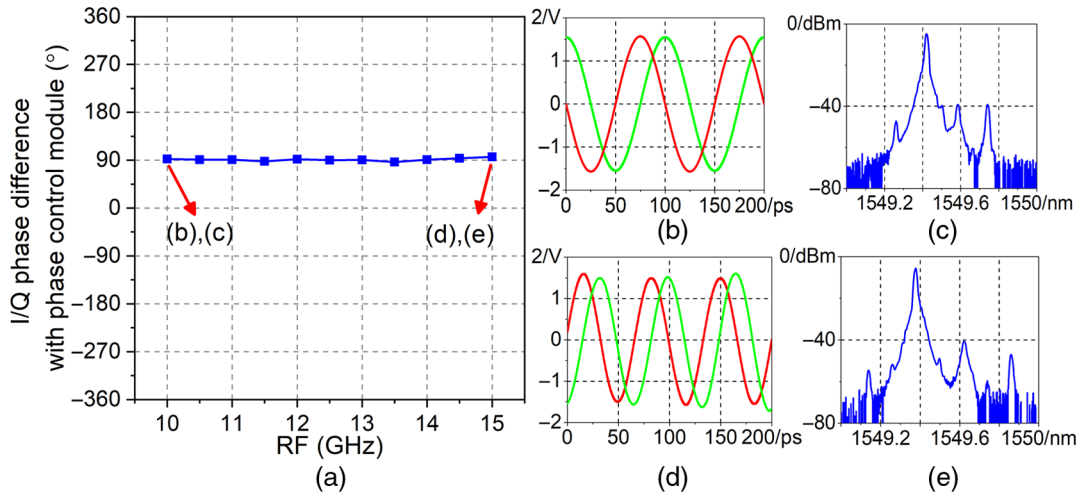


Fig. 5 I/Q phase difference and optical spectrum with phase control module: (a) I/Q phase difference when RF frequency changes from 10 to 15 GHz, (b) RF time-domain signal at 10 GHz, (c) optical spectrum after first RT at 10 GHz, (d) RF time-domain signal at 15 GHz, and (e) optical spectrum after first RT at 15 GHz.

3 Experimental Results

Experimental setup is shown in Fig. 6, the center wavelength of seed light source runs at 1549.5 nm, which is generated by an external cavity laser with the typical linewidth of 25 kHz. After injected in a 50:50 coupler, the seed lightwave is sent to an I/Q modulator with insertion loss less than 5 dB. RF signal generator with the frequency range from 10 MHz to 18 GHz is used to generate the sinusoidal signal, which is fed into a phase control module; the improved module works adaptively and outputs two RF driven signals with $\pi/2$ phase shift automatically; the amplitudes of the driven signals are carefully adjusted by two tunable electrical amplifiers to ensure equal power. For the purpose of making the I/Q modulator locked in SSB state, the output of the modulator is sent to a 1:99 coupler, whose 1% output port is connected to a modulator bias controller (MBC), it can implement automatic bias control and two DC bias voltages are locked at null points. A flat-top shape OBPF with 3-dB bandwidth of 3 nm is launched in the loop to select the required frequency window, and the center wavelength of OBPF is set to 1548 nm. To compensate for the insertion loss of the I/Q modulator and the filter, an EDFA with low noise figure has

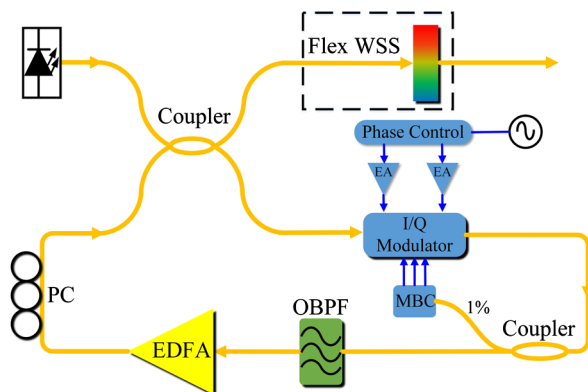


Fig. 6 Experimental setup of the proposed dynamic RFS.

been applied, which provides a saturation output power of 23 dBm.

At first, RF tone frequency is set to 12.5 GHz, as shown in Fig. 7, we successfully generate 30 stable carriers, the result is observed using the optical spectrum analyzer YOKOGAWA AQ6370D with a resolution of 1 pm. With the help of MBC, the I/Q modulator works stably at SSB condition to induce a 12.5-GHz frequency shifting to the input optical signal; $\lambda_0 = 1549.5$ nm represents the wavelength of seed laser and λ_{29} is 1546.6 nm; the carrier number is restricted due to the limited bandwidth of OBPF; and the generated stable 30 carriers have superior performance with 1.3-dB flatness fluctuation and above 54.2 dB carrier-to-noise ratio (CNR).

To verify the effectiveness of the proposed scheme, with the combination of the SSB-RFS and the improved module, we achieve variable interval optical carriers with dynamic RFS. When RF is changed from 12.5 to 10 GHz and anything else has not been adjusted, as shown in Fig. 8(a), 38 carriers in 3-nm bandwidth are obtained. The measured CNR value is about 53.9 dB with 1.5-dB flatness fluctuation;

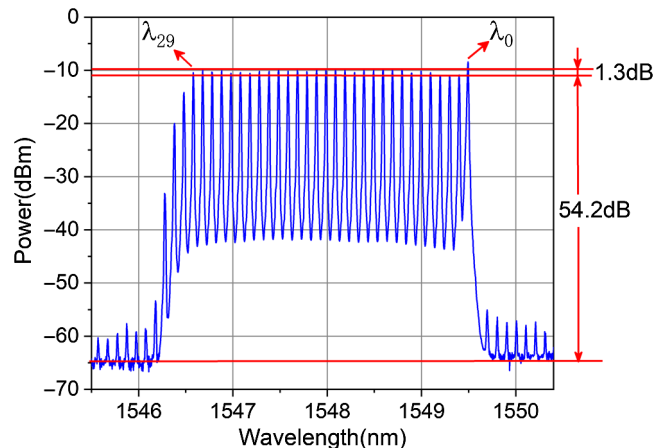


Fig. 7 30 stable frequency-locked-carrier spectrum with 12.5-GHz interval.

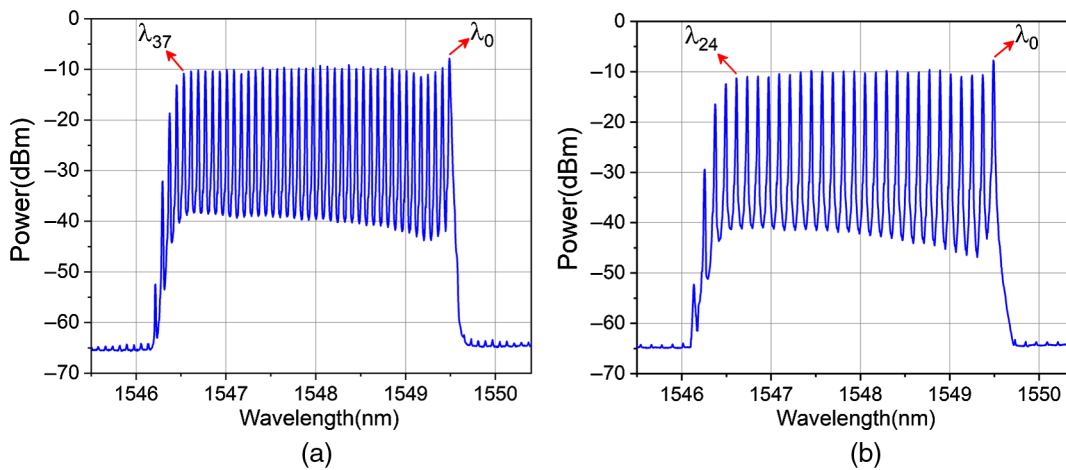


Fig. 8 Multicarrier generation with: (a) 10-GHz interval and (b) 15-GHz interval.

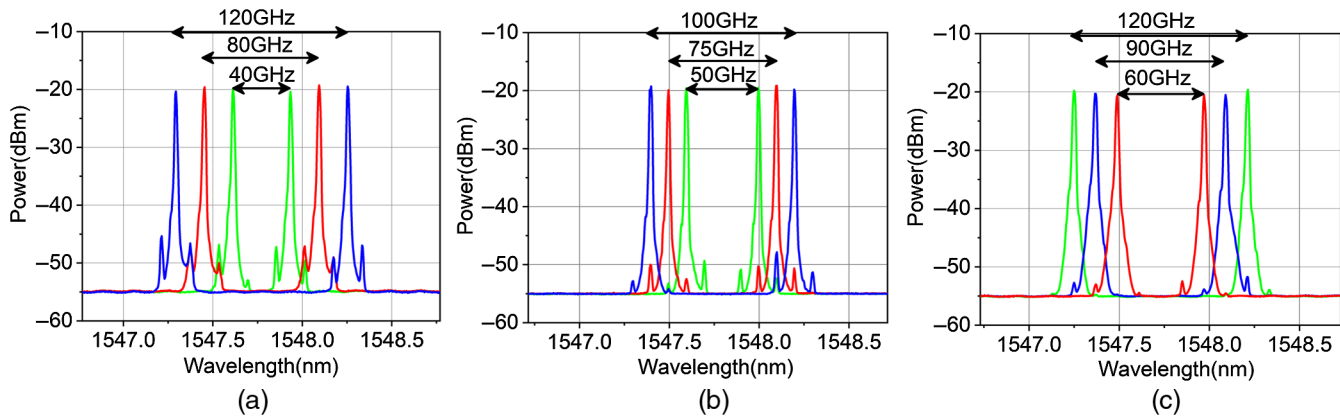


Fig. 9 Optical spectrum after WSS with RF set to: (a) 10 GHz, (b) 12.5 GHz, and (c) 15 GHz.

then RF is changed to 15 GHz, as shown in Fig. 8(b), 25 optical carriers are obtained with 54.7-dB CNR and 0.8-dB flatness fluctuation, where we can find that the results showing negligible CNR and flatness loss by using the proposed scheme.

By implementing a flexible wavelength selective switch (WSS) after the generation of flexible interval multicarriers, carriers with arbitrary intervals can be achieved. The flexible WSS is implemented by a programmable optical processor (WaveShaper 16000S). Experimental results are shown in Fig. 9, carriers with 40-/80-/120-GHz interval are obtained when RF is set to 10 GHz in dynamic RFS, carriers with 50-/75-/100-GHz interval are obtained when RF is set to 12.5 GHz, and when RF is set to 15 GHz, carriers with 60-/90-/120-GHz interval are obtained after WSS. Therefore, carriers with arbitrary intervals can be achieved with the proposed scheme, which is very suitable for WDM-PON integrated with radio-over-fiber (ROF) and photon frequency hopping radar.

4 Conclusion

In this paper, the principle of flexible interval multicarrier generation with SSB-RFS is analyzed and a time-frequency-varying multicarrier generation configuration with phase control module is proposed. Experimental

demonstration is also carried out, flat and stable multicarriers with the variable interval from 10 to 15 GHz can be achieved, and results show that negligible CNR and flatness loss is induced by using the proposed scheme. With dynamic RFS and a flexible WSS, carriers with arbitrary intervals can be achieved. The outcomes will pave the way to support spectrum flexible optical transmission, WDM-PON, and photon frequency hopping technology.

Acknowledgments

This work is partly supported by National Natural Science Foundation of China (NSFC) (Grant Nos. 61675033/61425022/61727817/61835002/61775237/61522501); Beijing Nova Program (Grant No. Z141101001814048); the Fundamental Research Funds for the Central Universities (Grant No. 2014RC0203) and Fund of State Key Laboratory of IPOC (BUPT).

References

1. J. Li et al., "Improving the spatial resolution of an OFDR based on recirculating frequency shifter," *IEEE Photonics J.* 7(5), 1–10 (2015).
2. U. Rahat et al., "Pulsed laser-based optical frequency comb generator for high capacity wavelength division multiplexed passive optical network supporting 1.2 Tbps," *Opt. Eng.* 55(9), 096106 (2016).

3. Y. Ma et al., “1-Tb/s single-channel coherent optical OFDM transmission over 600-km SSMF fiber with subwavelength bandwidth access,” *Opt. Express* **17**(11), 9421–9427 (2009).
4. K. Kashiwagi et al., “Direct generation of 125-GHz-spaced optical frequency comb with ultrabroad coverage in near-infrared region by cascaded fiber configuration,” *Opt. Express* **24**(8), 8120–8131 (2016).
5. J. Pfeifle et al., “Coherent terabit communications with microresonator Kerr frequency combs,” *Nat. Photonics* **8**(5), 375–380 (2014).
6. Z. Wu et al., “Optical frequency comb generation through quasi-phase matched quadratic frequency conversion in a micro-ring resonator,” *Opt. Express* **20**(15), 17192–17200 (2012).
7. X. Li and J. Xiao, “Flattened optical frequency-locked multi-carrier generation by cascading one EML and one phase modulator driven by different RF clocks,” *Opt. Fiber Technol.* **23**, 116–121 (2015).
8. J. Li et al., “Theoretical and experimental study on generation of stable and high-quality multi-carrier source based on re-circulating frequency shifter used for Tb/s optical transmission,” *Opt. Express* **19**(2), 848–860 (2011).
9. F. Tian et al., “Generation of 50 stable frequency-locked optical carriers for Tb/s multicarrier optical transmission using a recirculating frequency shifter,” *J. Lightwave Technol.* **29**(8), 1085–1091 (2011).
10. X. Wang and M. Shayan, “Performance comparisons between semiconductor and fiber amplifier gain assistance in a recirculating frequency shifter,” *Opt. Lett.* **43**(5), 1011–1014 (2018).
11. J. Lin et al., “Low noise optical multi-carrier generation using optical-FIR filter for ASE noise suppression in re-circulating frequency shifter loop,” *Opt. Express* **22**(7), 7852–7864 (2014).
12. X. Li et al., “Multi-channel multi-carrier generation using multi-wavelength frequency shifting recirculating loop,” *Opt. Express* **20**(20), 21833–21839 (2012).
13. L. Sun et al., “Performance analysis on quality of optical frequency comb generated by the recirculating frequency shifter based on linear IQ modulator,” *Opt. Eng.* **54**(11), 116106 (2015).
14. X. Li et al., “Performance analysis of the dual-parallel polarization modulator based optical single-sideband modulator/frequency shifter,” *Opt. Eng.* **55**(6), 066116 (2016).
15. L. Sun et al., “High order SSB modulation and its application for advanced optical comb generation based on RFS,” *Opt. Commun.* **354**, 380–385 (2015).

Zhipei Li received his BS degree in communications and information engineering at Harbin Engineering University, Harbin, China, in 2013. He is currently pursuing his PhD degree in electronic science and technology at Beijing University of Posts and Telecommunication,

Beijing, China. Now, he is engaged in research on high-speed fiber communication systems, including multicarrier transmission, high-order modulation formats, DSP algorithms in coherent systems, and multidimensional multiplexing technology.

Bo Liu received his bachelor's degree in 2008 at Beijing University of Posts and Telecommunications (BUPT), and completed his master's and PhD degrees from 2008 to 2013 in optical engineering in BUPT. He is currently a professor with the School of Physics and Optoelectronics, NUIST, China. His research interests include all-optical signal processing, radio over fiber, and broadband optical communication.

Qi Zhang received her PhD degree from BUPT, Beijing, China, in 2005. Currently, she is a professor at the School of Electric Engineering at BUPT. Her main research interests focus on optical communication and satellite communication.

Xishuo Wang is working for his PhD at Beijing University of Posts and Telecommunications. He received his BS degree in electronic science and technology from Beijing University of Posts and Telecommunications in 2018. His current research interests include coherent optical communication systems, radio over fiber systems, and signal shaping.

Yaya Mao received her bachelor's and PhD degrees from Nanjing Normal University and Beijing Jiaotong University in 2003 and 2017, respectively. She is currently an associate professor with Optoelectronics Research Institute, NUIST, China. Her current research interests include optical communication and all signal processing.

Xiangjun Xin received his PhD degree from the School of Electric Engineering, BUPT, Beijing, China, in 2004. Currently, he is a professor at the School of Electric Engineering and a member of the State Key Laboratory of Information Photonics and Optical Communications in BUPT. His main research interests focus on broadband optical transmission technologies, optical sensors, and all-optical networks. Within this area, he has published more than 60 Science Citation Index papers.